International Journal of Mining Science and Technology 24 (2014) 871–881

Contents lists available at ScienceDirect

International Journal of Mining Science and Technology

journal homepage: www.elsevier.com/locate/ijmst

# Distinct element modelling of fracture plan control in continuum and jointed rock mass in presplitting method of surface mining

Sharafisafa Mansour [a,*], Aliabadian Zeinab [a], Alizadeh Rezvan [b], Mortazavi Ali [a]

[a] Department of Mining, Metallurgy and Petroleum Engineering, Amirkabir University of Technology, Tehran, Iran
[b] Department of Mining Engineering, Sahand University of Technology, Tabriz, Iran

ARTICLE INFO

*Article history:*
Received 17 February 2014
Received in revised form 20 April 2014
Accepted 22 June 2014
Available online 15 November 2014

*Keywords:*
Controlled blasting
Presplitting method
Continuum and jointed rock mass
Distinct element modelling

ABSTRACT

Controlled blasting techniques are used to control overbreak and to aid in the stability of the remaining rock formation. Presplitting is one of the most common methods which is used in many open pit mining and surface blast design. The purpose of presplitting is to form a fracture plane across which the radial cracks from the production blast cannot travel. The purpose of this study is to investigate of effect of pre-splitting on the generation of a smooth wall in continuum and jointed rock mass. The 2D distinct element code was used to simulate the presplitting in a rock slope. The blast load history as a function of time was applied to the inner wall of each blasthole. Important parameters that were considered in the analysis were stress tensor and fracturing pattern. The blast loading magnitude and blasthole spacing and jointing pattern were found to be very significant in the final results.



## 1. Introduction

Drilling and blasting continues to be an important method of block production and block splitting. Drill and blast technique has a disadvantage that sometimes it produces cracks in uncontrolled manner and also produces micro cracks in the block as well as in remaining rock, if not carefully carried out. Recovery by this method is low as compared to other methods. Therefore, attempts have been made to develop controlled growth of crack in the desired direction. The control of fractures in undamaged brittle materials is of considerable interest in several practical applications including rock fragmentation and overbreak control in mining [1–3]. One way of achieving controlled crack growth along specific directions and inhibit growth along other directions is to generate stress concentrations along those preferred directions. Several researchers have suggested a number of methods for achieving fracture plane control by means of blasting. Fourney et al. suggested a blasting method which utilizes a ligamented split-tube charge holder [4]. Nakagawa et al. examined the effectiveness of the guide hole technique by model experiments using acrylic resin plates and concrete blocks having a charge hole and circular guide holes [5]. Katsuyama et al. suggested a controlled blasting method using a sleeve with slits in a borehole [6].

Mohanty suggested a fracture plane control technique using satellite holes on either side of the central pressurized hole, and demonstrated its use through laboratory experiments and field trials in rock [7–8]. Nakamura et al. suggested a new blasting method for achieving crack control by utilizing a charge holder with two wedge-shaped air cavities [9]. Ma and An conducted a numerical study to investigate the effective parameters on propagation such as nearby to free face, pre-existing stresses as well as notched and guide hole and pre-split charge holders. They concluded that when the pre-existing joint is parallel to the free face, the block behind the joint will be well fragmented due to the free face. When the pre-existing joint is normal to the free face, there is no damage in the block behind the joint. It justifies the pre-splitting technique, which is designed to prevent overbreak. They also showed that charge holder is effective in controlling the initiation and propagation of fractures. Two-slit charge holder can be used in pre-splitting operation, while three-slit charge holder can be applied in smooth blasting where more fragmentation is desired at one side of the fractured plane [10].

Nakamura performed model experiments to examine the effectiveness of the guide hole with notches [11]. Cho et al. performed experiments using a notched charge hole to visualize fracturing and gas flow due to detonation of explosives [12]. Recently model experiments using PMMA specimens and electric detonators were carried out to observe the propagation of cracks between two charge holes in blasting by Nakamura et al [13]. The applicability of the guide hole method using a circular hole having two notches

* Corresponding author. Tel.: +98 61451541001.
*E-mail address:* msharafisafa@gmail.com (M. Sharafisafa).

http://dx.doi.org/10.1016/j.ijmst.2014.10.022
2095-2686/

between the charge holes was examined. Cho et al. used a numerical toll to study crack growth in notched hole and in models with guide holes [14]. They also studied fracture processes in laboratory-scale blasting of PMMA. Their study showed that predominant radial cracks propagate along different directions with different distribution patterns and the propagation direction affects the co-linearity of the fracture plane between the charge holes. They also showed that the propagation velocity of the opening crack decreased as the applied fracture energy Gf increases. Sharafisafa and Mortazavi studied fracture plane control in continuum media using numerical modelling [15]. They evaluate parameters which are effective in fracture propagation in presplitting controlled blasting such as spacing between blastholes and blast loading magnitude. Their study showed that these parameters are very significant in length and pattern of generated fractures around the blastholes as well as link between fractures to form a continuous crack.

Controlled blasting techniques produce the macrocrack in a desired direction and eliminate microcrack in the remaining rock. Macrocrack development in desired direction is required for extraction of dimensional stone and at the same time there is need to reduce microcrack development in the block and remaining rock. Blasting techniques have been developed to control overbreak at excavation limits. Some techniques are used to produce cosmetically appealing final walls with little or no concern for stability within the rock mass. Other techniques are used to provide stability by forming a fracture plane before any production blasting is conducted. On permanent slopes for many civil projects, even small slope failures are not acceptable, and the use of controlled blasting to limit damage to the final wall is often required. The principle behind these methods is that closely spaced parallel holes drilled on the final face are loaded with a light explosive charge that has a diameter smaller than that of the hole [14]. There are four methods of controlled blasting, and the one selected depends on the rock characteristic and the feasibility under the existing conditions. The four methods are line drilling, cushion blasting, smooth-wall blasting and presplitting (also pre-shear) [15].

Line drilling involves drilling holes precisely along the required break line at a spacing of two to four holes diameters, and then leaving a number of unloaded holes between the loaded holes. Line drilling is only used where very precise wall control is needed, such as corners in excavations. In another study, Sharafisafa and Mortazavi studied effect of a fault on wave propagation [16]. This study demonstrated the effect of presence of a fault on volume and length as well as direction of fractures. A major discontinuity such as a fault can arrest the fractures and as a result, fracture plane cannot fully form, which will result in incomplete presplitting blast. Rathore and Bhandari studied some effective parameters on fracture growth by blasting such as variation of explosive energy, variation of stemming, blasthole liners and so on [17]. Their result showed the variations of extent and direction of fractures with variation of mentioned parameters. For example, they concluded that by using notched hole with liner, crack was developed in desired direction and damages were controlled in extracted block and remaining rock.

When the rock is reasonably competent, smooth-wall blasting techniques can be used to advantage in underground applications. Horizontal holes are charged with small-diameter low-density decoupled cartridges strung together and by providing good stemming at the collar of the hole. Charges are fired simultaneously after the lifters. If the rock is incompetent, smooth-wall blasting may not be satisfactory [18]. Cushion and presplitting blasting are the most commonly used methods, with the main difference between the two beings that in cushion blasting the final row holes are detonated last in the sequence, while in pre-shearing the final line holes are detonated first in the sequence. Cushion blasting method is a control technique which is used to cleanly shear a final wall after production blasting has taken place. In cushion blasting method, the cushion holes are loaded with light, well-distributed charges. The sole purpose of a cushion blast is to create a cosmetically appealing, stable perimeter. It offers no protection to the wall from the production blast [14]. Presplitting consists of creating a plane of shear in solid rock on the desired line of break. It is somewhat similar to other methods of obtaining a smoothly finished excavation, but the chief point of difference is that presplitting is carried out before any production blasting and even in some cases before production drilling [4]. Presplitting utilizes lightly loaded, closely spaced drill holes, fired before the production blast. The purpose of presplitting is to form a fracture plane across which the radial cracks from the production blast cannot travel. Secondarily, the fracture plane formed may be cosmetically appealing and allow the use of steeper slopes with less maintenance. Presplitting should be thought of as a protective measure to keep the final wall from being damaged by the production blasting [18].

The presplit theory is that two simultaneously fired holes emit shock waves, which, when they meet within the web, place the web in tension, causing cracks and shearing it. Fig. 1 illustrates the presplit theory. In extremely weathered material, presplitting may have to be done at very close spacing with a very small amount of explosive. Presplit holes must be stemmed with an increased bottom charge to move the toe [19]. After detonation in presplit holes, waves generated from each hole propagate in a spherical shape and cracks are generated around holes.

Fig. 2 shows a presplitting blast project and rock shearing and forming the fracture plane in presplitting method. As can be seen from Fig. 2a, presplit blast leads to generate a fracture plane parallel to free face which is final wall of temporary slope. Fig. 2b illustrates a successful presplit blast with no unwanted damage in other sides. In order to operate a successful presplit

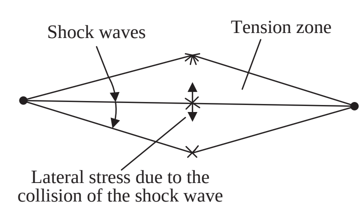


**Fig. 1.** Presplit principle [20].

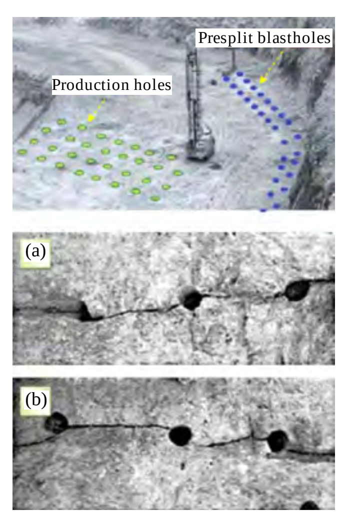


**Fig. 2.** Fracture patterns in the presplitting blast method (a) location of presplit holes and production holes; (b) final fracture plane after presplit blast [21].

blast, significant factures involved in rock blasting should be noted and calculated properly. Knowing the blasting mechanism in rocks can be helpful in the design process of rock blasting. Fractures initiated from holes propagate around hole in main three fractured zones. These three zones are crushed zone, severely fractured zone and incipiently cracked zone. In presplitting blast method, the main emphasis is placed on incipiently cracks which are the major cracks in rock blasting process. The extension of three blast zones in presplit holes depends on the spacing between blast holes and explosive load. Therefore, in this study the spacing between blast holes and the explosive load are discussed as the governing parameters.

In order to investigate the effects of significant parameters involved in presplitting blast method, numerical tools was applied in this study. There are some numerical tools available for blasting in rock masses at present, the most widely used being the finite element method (FEM), boundary element method (BEM), finite difference method (FDM), and discrete element method (DEM), etc. The efficiency of DEM in blast and wave and fracture propagation was discussed in some studies. Khan employed rapid failure of a test rock specimen under cylindrical tensile wave effect [22]. The study concluded that DEM can be efficient to solve dynamic problems of rock mechanics or to control chronologically stress-strain state (SSS) of a material. Aliabadian et al. employed 2D distinct element code to study the effect of in-situ stresses and loading rate on blasting induced fracture propagation [23]. They showed that distinct element method can simulate the fracture propagation and wave attenuation in dynamic analysis in agreement with reality. Therefore, in present study, two-dimensional discrete element code which is capable to simulate the responses of rocks subjected to either static or dynamic loadings was used.

## 2. Numerical modelling procedure

Numerical codes are useful tools to build models of complex problems, which have complex geometry, loading condition and boundary condition. The rock-explosive interaction in multi-row blasting operations is an example of such problems. The experimentation of such problems is very difficult, expensive and not easily doable in the actual field scale. On the other hand, sophisticated codes enable handling of dynamic behavior, complex geometries and nonelastic material behavior. Numerical methods, once calibrated with practical experiments and observations, can be used for parametric studies aimed at analyzing the effect of critical parameters on the structure response. It is the goal of this section to look into the effects of important parameters involved in presplitting blast method.

## 3. Modelling strategy and input data

As pointed out in the previous sections the goal of this work was to look into the effects of important parameters involved in presplitting blast. Employing the commercial numerical code, a 2D model of a typical block was constructed. Fig. 3 illustrates an overall view of the model. Identical holes of 10 cm in diameter and in 0.5, 1, 2, 3 and 4 m in distance were considered. Further details of the blast geometry are shown on the figure. Since the objective of the study was to look at the problem from stress/failure mechanism point of view, the Mohr-Coulomb material model was used to model the rock mass behavior. The problem can be treated as a plane-strain case, in which the $X$- and $Y$-axis lie on the vertical plane with the origin at the centre of the model.

In Fig. 3, $D$ is the distance between holes in different calculation models. All boundaries were considered as viscous boundaries (non-reflecting) to eliminate wave reflection. It should be noted

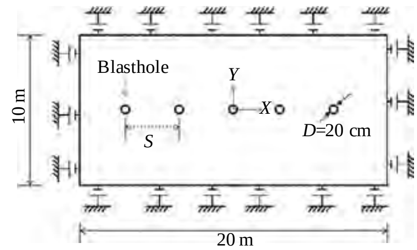


**Fig. 3.** Overall view of the model.

that the number of holes depends on the spacing between holes in the model and Fig. 3 just shows an overall view of model. The rock type was assumed to be diorite [24]. The materials properties used are shown in Table 1.

In order to estimate the pressure from the charge, experimental methods can be helpful. The magnitude of shock wave pressure is a function of velocity of detonation, density and charge's ingredients [19].

Although this relation is very complicated, but the following equation can estimate blast load:

$$PD = 432 \times 10^{-6} \frac{\rho_e . VD^2}{1 + 0.8\rho_e} \tag{1}$$

where $PD$ is blast pressure (MPa); $\rho_e$ explosive density (g/cm$^3$) and $VD$ velocity of detonation (m/s). Putting the dynamite properties in the above equation:

$$PD = 432 \times 10^{-6} \frac{1.45 \times 3000^2}{1 + 0.8 \times 1.45} = 2610 \text{ MPa}$$

Gas pressure usually is considered half of the blast pressure, e.g.:

$$PE = \frac{1}{2} PD = 1305 \text{ MPa} \tag{2}$$

If the diameter of the explosive is equal to blasthole's diameter, then there is no gap between blasthole and explosive and the related pressure can be calculated as follows:

$$PW = PE \cdot \left(\frac{r_h}{b}\right)^{-q\kappa} \tag{3}$$

where $r_h$ is hole radius (mm); $b$ explosive radius (mm), $\kappa$ specific heat coefficient, and $q$ shape factor of explosive (2 for cylindrical charges and 3 for spherical charges) [25]. Therefore:

$$PW = 1305 \left(\frac{38}{38}\right)^{-2\times1.2} = 1305 \text{ MPa}$$

On the other hand, applied dynamic pressure on blasthole's wall is a function of time because of interaction between rock and generated shock wave. Many experimental equations have been presented to calculate this parameter, but presented equations by Starfield and Pugliese and Duvall are widely used [26–27]. According to Starfield's equation, generated dynamic pressure on the wall ($P(t)$) is a function of rock density ($\rho_r$), explosive density ($\rho_e$), $P$-wave velocity ($C_p$), velocity of detonation ($VD$) and $PW$. The following equation gives $P(t)$:

$$P(t) = PW \cdot \frac{8\rho_r \cdot C_p}{\rho_r \cdot C_p + VD \cdot \rho_e} \left[e^{(-Bt/\sqrt{2})} - e^{(-\sqrt{2}Bt)}\right] \;\&\; B = 16338 \tag{4}$$

The explosive density ($\rho_e$) is 1.45 (g/cm$^3$). Therefore for quartzitic sandstone:

$$P(t) = 2350\left[e^{-11552.7t} - e^{(-\sqrt{32676t})}\right]$$

The Fig. 4 shows the graph drawn based on above equation.

**Table 1**
Rock mass properties used as input.

| Parameter | Density (kg/m$^3$) | Bulk modulus (GPa) | Shear modulus (GPa) | Tensile strength (MPa) | Shear strength (MPa) |
|---|---|---|---|---|---|
| Value | 3160 | 52.4 | 39.6 | 18.8 | 44.16 |

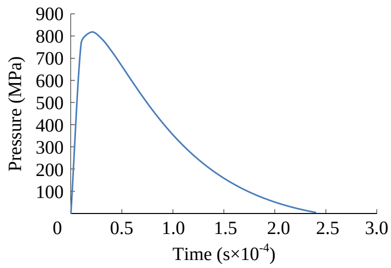


**Fig. 4.** Dynamic pressure applying on the blastholes's wall.

As can be seen from Fig. 4, the peak pressure is about 820 MPa. It was assumed that the explosive is of a shocky type and delivers most of its energy in the form of stress wave. It should be noted that the shape of stress pulse presented in Fig. 4 was used in first step of calculations which were conducted to investigate the spacing effect between holes. The second step of calculations was evaluating the effect of the amount of pressure applied to holes with the same rise and fall times. In order to better understanding of wave propagation in presplitting method, plasticity indicators and velocity vectors were monitored as a function of stress wave propagation/collision in each model and for comparing the results, the monitored parameters were plotted at the same time. Moreover, history locations were considered at points between holes as well as in locations lying parallel to $Y$-axis around each hole.

## 4. Numerical simulation results of spacing effect on fracture plane creation

As outlined earlier, five models consist of five different distances between holes ($S$ = 0.5, 1, 2, 3 and 4 m) were conducted. All models have the same dimensions in width and length as presented in Fig. 3. Main difference in the models is in number of holes which depends on the distance between holes. After static calculation, dynamic analysis of the applying the blast load on blasthole's wall was conducted. Fig. 5 illustrates velocity vectors as wave front propagating in the rock mass in five models mentioned earlier. As can be seen in Fig. 5, each model has different trend of wave propagation and collision from others. In the cases of 0.5, 1 and 2 m in $S$, before 0.2 ms the wave fronts from each hole collide one another and complicated interaction between wave fronts starts, whereas in the cases of 3 and 4 m in $S$, wave fronts have not collided two wave fronts raised from adjacent blastholes. These interactions between wave fronts lead to different fracture pattern of rock mass in each model. Fig. 6 illustrates rock failure and crack propagation in 5 mentioned model.

As can be seen from Fig. 6, fracturing in each model has different trend from others which indicates effect of different distance between holes. As mentioned earlier in Section 1, depends on distance between holes, different types of blast induced fracturing are generated around holes. Once the spacing is too close, numerous fractures link in the plane between holes and when the blast is excavated the material between holes will fall out leaving half casts protruding from the final wall. Moreover, the most yielded zones are crushed zones and other types of fractures such as severely fractured zone and incipiently cracked zone are not created. This fracturing pattern indicates less damage to adjacent walls and forming a straight fracture plane. This process can be seen in Fig. 6 and in models with 0.5 and 1 m in spacing. Increasing in spacing leads to generate longer fractures as well as decreasing crushed zone's area. If spacing is more than 2 m and less than 4 m, severely fractured zone will be dominated fracture zone and crushed zone will be restricted just in close distances around holes. These fractures link in the plane between holes and lead to generate a fracture plane which is the desired fracture plane. On the other hand, incipiently fractures generated from cracked zone are too short to form linked cracks which means in these spacings wave fronts interference is just able to generate short cracks. Furthermore, fractures initiated from crushed zone lead to damage to adjacent walls. Therefore, if spacings are too far, a face that is generally rough in appearance will result. In the cases with very large distance between holes, wave front generated from each hole acts similar to an individual blast in rock mass and complete fracture process zone around blastholes is generated which consists of crushed zone, severely fractured zone and incipiently cracked zone. This phenomenon means there is no constructive or unconstructive interference between stress wave fronts and rock failure is limited just around blastholes. Therefore, fractures initiated from blastholes do not link together which means there is no fracture plane and applicability of presplit blast is not fulfilled. As can be observed from Fig. 6 in the case of $S$ = 4 m, fracture plane has not generated and just longer fractures propagate around blasthole.

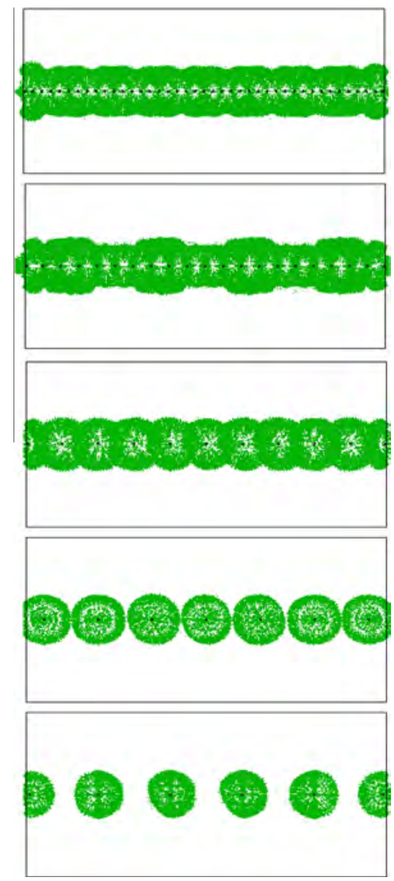

**Fig. 5.** Illustration of stress wave front at 0.2 ms ($S$: Spacing).

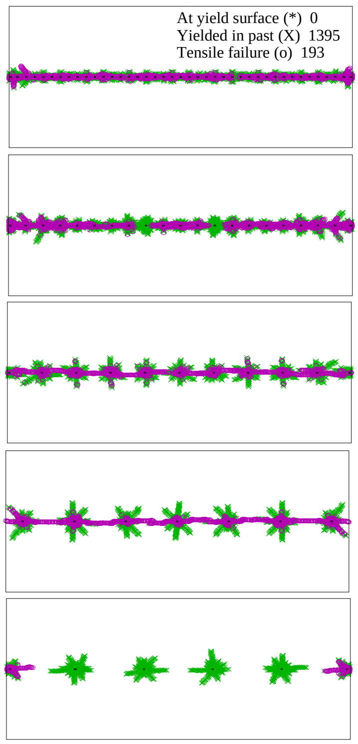


**Fig. 6.** Rock mass failure and crack propagation under blast loading.

In order to evaluate the stress states and the role of these stresses in rock mass breakage subjected to blast load, history locations were considered between holes to record stresses. Considering the paper scope, more meaningful parameters (e.g., *xx*-stress, *xy*-stress and *yy*-stress) were extracted and presented here to compare the differences in stresses state in each model. Fig. 7 illustrates the variation of $S_{xx}$, $S_{yy}$ and $S_{xy}$ at halfway points between two blastholes.

As can be observed from Fig. 7 three graphs have the same trend and increase in the spacing leads to decrease in stress level. On the other hand, there is a big difference between *xx*-stress and other two stresses. The maximum *yy*-stress is about 17.85 MPa and for shear stress (e.g., *xy*-stress) is about 2.9 MPa, whereas the maximum value for *xx*-stress is approximately 122 MPa. These levels of stresses mean that $S_{xx}$ is the major stress and responsible for rock mass failure. Looking at Fig. 7, 2 m in the spacing is the critical spacing and spacings less than 2 m lead to higher rate of energy delivery to the rock mass which cause to severely rock failure in the space between holes. This phenomenon was described earlier in the description of Fig. 6 which indicates good agreement between stresses state and the rock failure pattern. Once the spacing is smaller than 2 m, higher levels of stress leads to generate crushed zone around holes that is due to high and fast delivery of energy to the rock mass. Moreover, constructive interference of stress waves generated from each hole leads to higher fragmentation locally. In the case of 4 m spacing, maximum *xx*-stress, *yy*-stress and *xy*-stress are about 10, 1.3 and 0.127 MPa, respectively. These magnitudes of stresses at halfway point between blastholes are disable to plastic failure of rock mass. Therefore, fractures initiated from holes cannot link together to generate a continuous fracture plane.

To further evaluate the issue the variations of $S_{xx}$, $S_{yy}$ and $S_{xy}$ along blasthole center line parallel to *Y*-axis at a distance of 40 cm were measures and the results are plotted in Fig. 8. This figure shows crack evolution around blastholes which depends on spacing.

This figure indicates that the most significant stress component is the $S_{yy}$ with maximum magnitude in the spacing of 4 m. The trends shown in figure above indicate that propagation of fractures initiated from blastholes are due to *yy*-stress component and two other stresses (e.g., $S_{xx}$ and $S_{xy}$) can contribute to extend fractures. Shear stresses are too low to fail the rock mass and do not have effective role in the rock mass failure. On the other hand, in the spacing more than 1 m, there is an opposite trend between $S_{xx}$ and $S_{yy}$. Increasing the distance between holes causes a uniform distribution of energy in the rock mass around blasthole and to generate a complete fracture process zone that unwanted damage to the adjacent wall of the blasthole will result. In the early milliseconds of detonation $S_{yy}$ causes compressive failure of the rock mass and after these times $S_{xx}$ causes tensile stress concentration at the tips of cracks which will extend the cracks. Tensile stress concentration at crack's tips leads to propagate the cracks to the undesired directions and unwanted fragmentation of the rock mass.

Fracture propagation is mainly dependent to spacing between blastholes, so that final wall will be generated in rough or flat. Fig. 9 shows a schematic and numerical illustration of fracture propagation and final wall generation at the cases with close and large spacings.

As can be observed from Fig. 9, if blastholes are overloaded or spacing is close, crushing of the blasthole wall will result. If spacings are too far, a face that is generally rough in appearance will result.

## 5. Effect of blast loading magnitude on fracture pattern

The dynamic responses of a rock mass to blasting are much affected by loading magnitude of the explosive charge, which may influence the rock fracture pattern. In order to investigate the effect of loading magnitude on the fracture pattern, five pressure wave pulse with maximum pressures equal to 300, 400, 500, 600 and 700 MPa and the same rise and fall times as Fig. 4 were adopted in the numerical simulation. These pressure wave pulses were applied to a model with 4 m spacing to better illustration of rock failure. The general model is same as Fig. 3. Fig. 10 illustrates rock mass failure subjected to different blasts loadings.

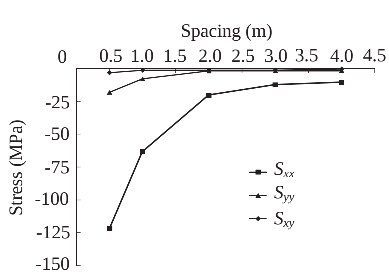


**Fig. 7.** Histories of maximum stresses at halfway between two blastholes.

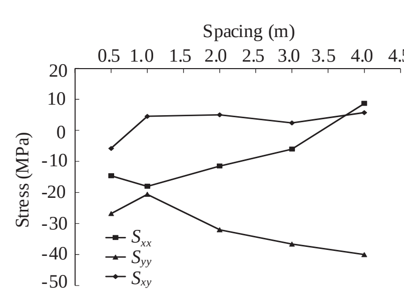


**Fig. 8.** Histories of maximum stresses along blasthole center line.

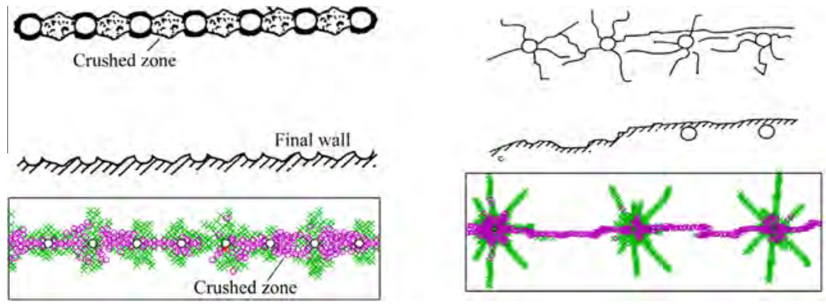


**Fig. 9.** Generation of final wall at close and large spacing.

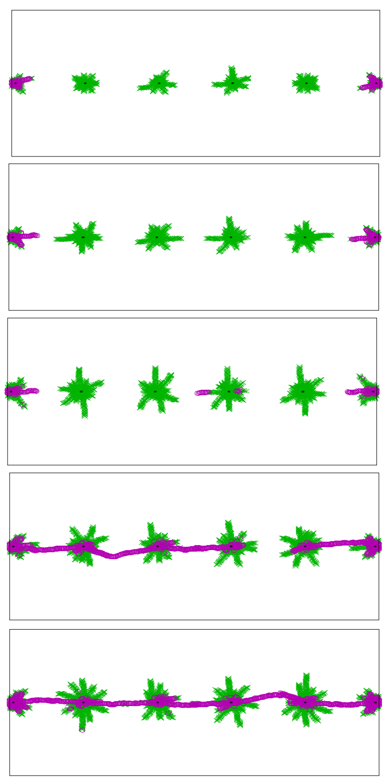

**Fig. 10.** Illustration of rock failure subjected to five different blasts loading.

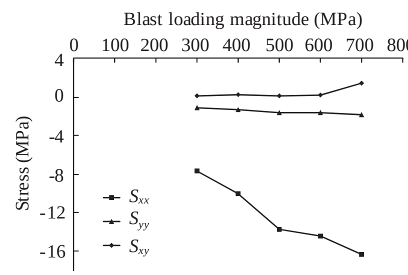


**Fig. 11.** Variation of $S_{xx}$, $S_{yy}$ and $S_{xy}$ at halfway point between blastholes.

As can be seen from Fig. 10, a higher loading magnitude increases the number of fractures and causes the intense stress release around the running fractures.

When the blast loading is less than 500 MPa, fractures generated from the blastholes cannot link together to generate a continuous fracture plane and fracture pattern is similar to blasting in a single blasthole. When blast loading exceeds 500 MPa, constructive interference of stress waves generated from each hole leads to higher fragmentation locally. This phenomenon occurs in points between holes and leads to link incipiently fractures which create final fracture plane. As can be seen from Fig. 9 in the case of 600 MPa, fractures are not linked together entirely and linked fractures have not generated a straight line which is desired. When the blast loading exceeds 600 MPa and reaches to 700 MPa, a perfect fracture plane is generated that is main scope of presplit blasting performance. It should be noted that intensive blast load leads to generate more fractures around hole which can damage rock mass around blasthole in unwanted directions. In order to investigate the stresses states at the points between holes, history points to record stresses were considered at these points. Fig. 11 shows the variation of $S_{xx}$, $S_{yy}$ and $S_{xy}$ at halfway points between two blastholes.

As illustrated in Fig. 11, there is a meaningful difference between $S_{xx}$ and other two stresses. With increasing the applied pressure on blasthole's wall, the *xx*-stress increase gradually. The red graph shows two trends. Firs trend begins at 7.65 and ends at 13.7 MPa, and the second trend is between 13.7 and 16.3 MPa. In the first trend rock failure does not occur in this point, whereas in the second trend rock failure occurs. This means that to generate a continuous fracture, 500 MPa is critical loading and blast loading should be increased to more than this value. On the other hand, *yy*-stress and *xy*-stress do not have significant effect on rock failure in this point which indicates that these stresses do not contribute to link fractures between holes.

Fig. 12 illustrates the variation of $S_{xx}$, $S_{yy}$ and $S_{xy}$ at a point along blasthole center line parallel to *Y*-axis at a distance of 40 cm. In this figure it is clear that at points along to blasthole center, rock failure is due to high values of *yy*-stress. There is a dramatic increase in the magnitude of *yy*-stress with increasing the blast loading. It means that *yy*-stress is responsible for creating fractures in directions parallel to *y*-axis. Therefore, mainly the *yy*-stress component leads to damage to rock mass in undesired directions. On the other hand, *xx*-stress and *xy*-stress have approximately remained constant and maximum value of *xx*-stress and *xy*-stress are about 10 and 5.6 MPa, respectively.

## 6. Blasthole diameter effect on generation of fracture plane

Hole diameter is one of most important parameter which effects on final fracture plane generation. To study this parameter on fracture propagation, seven models with 76, 100, 120, 140, 160, 180 and 200 mm in diameter of blastholes were built. Then, blast load was applied to blastholes and the results were extracted. Fig. 13 illustrates the fracture pattern at each model.

As can be seen from Fig. 13, increasing the diameter lead to increase in fracture extent. With a diameter of 200 mm, final fracture plane is generated, while with diameters lower than 200 mm, fracture generation and inking between fractures is local and con-

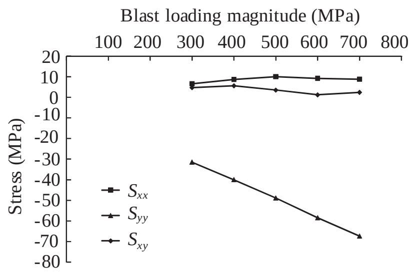


**Fig. 12.** Histories of $S_{xx}$, $S_{yy}$ and $S_{xy}$ along blasthole center line at a distance of 40 cm.

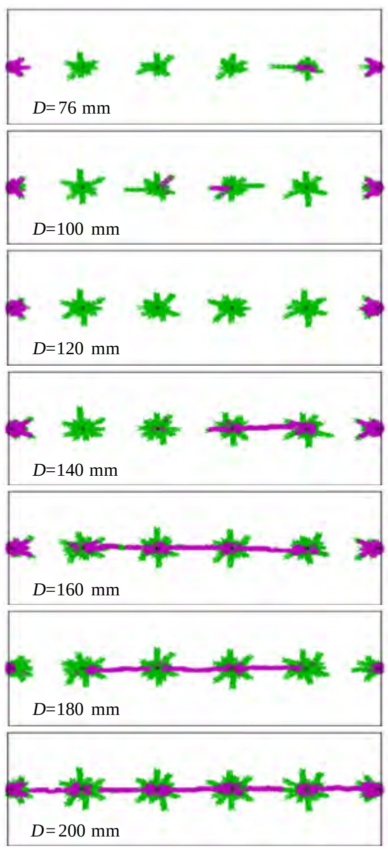


**Fig. 13.** Effect of hole diameter on fracture generation.

tinuous fracture plane is not generated. It should be notified that however increasing diameter will result in a continuous fracture plane which is the aim of presplitting method, excessive failure in directions perpendicular to blastholes axis will result in irregular plane generation of remained wall and final wall will be rough.

## 7. Presplitting method simulation in jointed a rock mass

To evaluate the effect of discontinuities on wave and fracture propagation in jointed rock masses, a study of distinct element was carried out. In this part, five models with different jointing pattern are discussed. These five models are: joints parallel to *x*-axis, joints perpendicular to *x*-axis, joint with 45° orientated respect to *x*-axis, random jointing and randomly polygonal joints (Voronoi jointing). Fig. 14 illustrates the mentioned models.

It should be noted that all parameters such as rock properties, blasthole's diameter, boundary conditions and blast loads are the same as previous section. Joint properties are shown in Table 2 [28]. After modelling each model, blast pressure was applied to blastholes. Fig. 15 shows final fracture plane generation in each model.

Fig. 15 clearly demonstrates difference in rock mass failure pattern in each model. When the joints are parallel to *x*-axis, at early times after detonation radial fractures are first initiated and propagated from the borehole surface without directional preference. After more wave propagation in the media, compressive wave collides to first set of joints and reflects as tensile wave. This tensile wave energy exceeds rock mass tensile strength and leads to tensile failure of rock at vicinity of joints. The generated cracks at the area between blasthole and joints cause to damage to remained wall as well as generation a rough surface which is undesirable in the formation of final fracture plane. These fractures are marked in Fig. 16 with red arrows. On the other hand, at the areas between two adjacent blastholes compressive waves collide each other at the same time after detonation of each hole and at point located at halfway between blastholes and constructive interference of waves leads to linking initiated fractures from each blastholes and a continuous fracture between blastholes is generated. This continuous fracture is marked with black arrow in Fig. 16. These fractures are the main aim of controlled blasting.

In the model with perpendicular joints to the *x*-axis, as can be seen, fracture propagation is restricted to the area between blasthole and immediate joint. The reasons for this phenomenon can be described as two, first is that especial spatial distribution of joints does not allow waves to across the joints and the joints cause wave reflection from their surface. The wave reflection leads to excessive failure of rock mass around the blasthole as well as nearby the joint surface, while no continuous fracture is formed between adjacent blastholes. In the other word, the joints arrest initiated fractures. This phenomenon is illustrated in Fig. 17 with red arrows. The second reason can be expressed as far distances between blastholes. When the spacing between blastholes is too far, transmitted waves energy will attenuate while propagating from rock mass and joints and as a result, cannot fail the rock mass at far distances. Therefore, at this kind of jointing patterns, spacing between blastholes should be optimized based on joint spacing. To demonstrate the effectiveness of decreasing spacing between blastholes in generation of continuous fracture plane, a model with 1 meter spacing between blastholes and with same jointing pattern as previous section was analysed.

The fracture propagation and generation of fracture plane is shown in Fig. 18. As can be seen from the figure, final fracture plane is generated in a desirable manner and damage to remained wall is the minimum. The magnified view of a part of model in Fig. 18 clearly demonstrates generation of continuous plane and also shows damage extension to remained wall. Although the remained wall is damaged by two fractures (marked with black arrows in Fig. 18), but the damage to remained rock mass is inevitable because wave reflection from joints will result in constructive and unconstructive interferences between incident and reflected waves and as a result, failure at some degrees will be occurred at the area between adjacent joints. To further evaluation of the issue the variation of $S_{xx}$ at halfway point between two adjacent joints and a distance of 0.5 m in *y*-direction was measured as a function of time. Fig. 19 shows the variation of *xx*-stress at the point. As can be observed, after 0.1 ms from detonation compressive wave collides joint and then reflects back into rock mass in tensile wave form. This wave again hits to another joint and this collision and reflection results in failure of rock mass at areas between two adjacent joints.

When joints are orientated 45° respect to blastholes alignment axis, the failure pattern and the shape of final remained wall differs from two previous mentioned models. In this case, initiated fractures from blastholes propagate in all directions and depend on

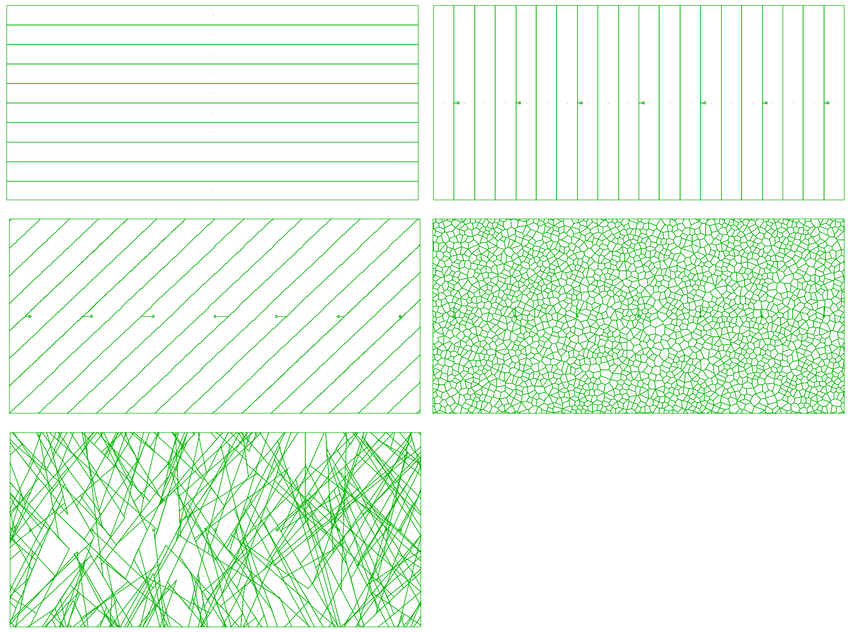

**Fig. 14.** Geometry of five models with different jointing pattern.

**Table 2**
Joint properties used as input [28].

| Parameter | Normal stiffness (GPa/m) | Shear stiffness (GPa/m) | Cohesion (MPa) | Friction angle (°) | Tensile strength (MPa) |
|---|---|---|---|---|---|
| Value | $k_n = 1.2$ | $k_s = 0.6$ | 0.3 | 36.2 | 0.029 |

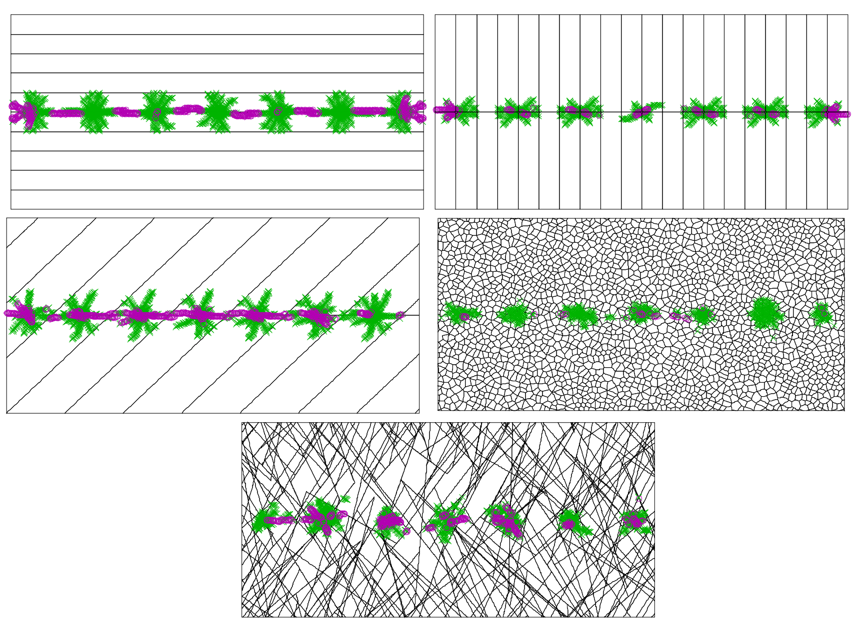

**Fig. 15.** Rock mass failure around blastholes in different jointing patterns.

the joint orientation, fractures link together in an irregular manner. Fig. 15c illustrates fracture evolution in the model with 45° orientated joints with respect to blastholes alignment axis. The figure clearly shows fracture linking between adjacent holes and generation of final fracture plane. To further studying the issue, a magnified view from Fig. 15c is shown in Fig. 20. Fig. 20a shows fracture propagation and rock mass failure around blastholes.

Fig. 20b illustrates numerical and schematic view of remained wall shape and generated rough surface. As can be seen, pre-split blasting at this case leads to generate an irregular surface and achieving a flat wall is not guaranteed. Special orientation pattern of joints causes complicated interferences between incident and reflected waves and this phenomenon leads to generate more fractures toward joints and less failure in the opposite sides. This type

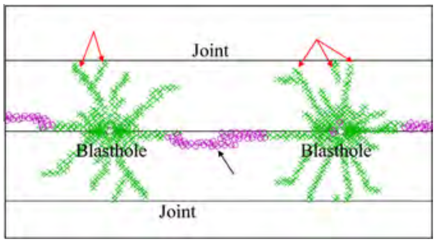


**Fig. 16.** Magnified view of fracture propagation around blastholes and joints.

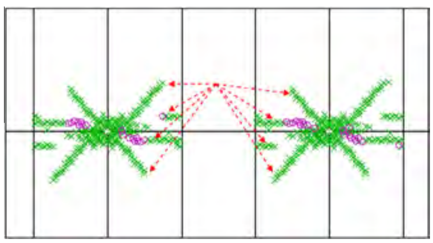

**Fig. 17.** A magnified view of rock mass failure around blastholes.

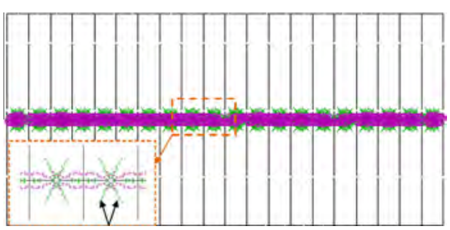

**Fig. 18.** Generation of fracture plane in blasthole spacing of 1 m.

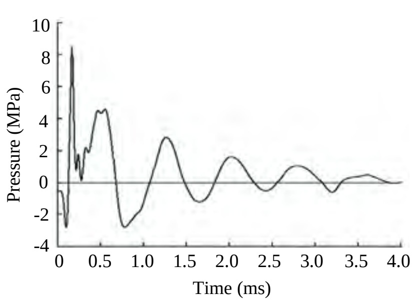


**Fig. 19.** Variation of $S_{xx}$ at halfway point between two adjacent joints.

of breakage, which leaves the half-cast protruding from the final face, would seem to indicate that blastholes are spaced too close and overloaded. Blastholes may be properly spaced, but the acute angles formed between the dominate joints and the face cause a different fracture pattern with two or more fracture linking between blastholes.

In this case, generation of fracture plane strongly depends on spacing between blastholes. In order to investigate the role of spacing on rock breakage, two different models (both with 45 degree orientated joints respect to blastholes alignment axis) were analyzed. Fig. 21 illustrates rock mass breakage in the models with 3 and 1.3 m spacing between blastholes. As can be clearly observed, when spacing is 1.3 m, initiated fractures from blastholes can link together to generate a continuous fracture plane as a accurate result of pre-split method, while when spacing is too far (3 m in this case) wave attenuation in the rock mass as well as reflection from the joints results in energy losing between blastholes and the low energy wave is disable to breakage rock mass at far distances. Therefore, final fracture plane is not formed and pre-split blasting operation is inefficient.

In the case of randomly polygonal joints (namely Voronoi joints) rock breakage pattern strongly depends on the shape of individual blocks. As shown in Fig. 15d, rock mass breakage is limited to blocks surrounding a blasthole. Fig. 22 shows a magnified view of breakage around blastholes.

Each block which is made by randomly polygonal joints treats as a closed area and arrests high energy waves and wave is attenuated in areas restricted in surrounding block of blasthole. Therefore, frequently collision and reflection from block boundaries leads to excessive breakage of rock mass into a block and adjacent block remain undamaged at the vicinity of the block. To generate a

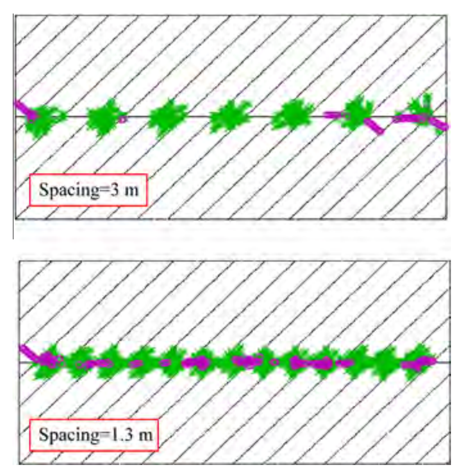


**Fig. 21.** Rock mass breakage pattern at two models with different spacing between blastholes.

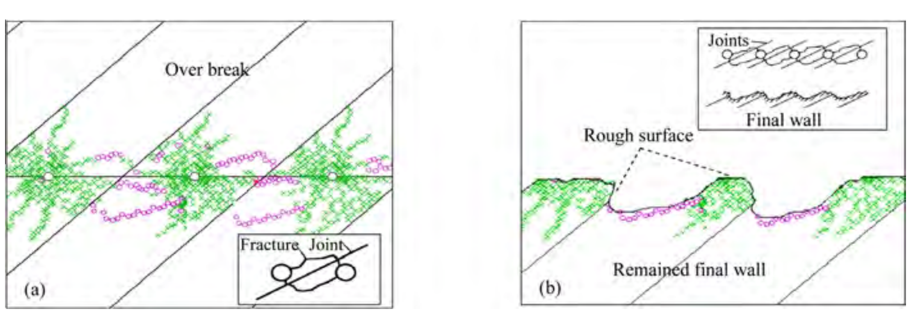


**Fig. 20.** Magnified view of fracture propagation between joints and generated rough wall.

continuous fracture plane in this case, it would be possible to change some controllable parameters such as hole diameter, blasthole's diameter, increasing in blast pressure. For instance, a model with increasing in blast load was simulated and the result is shown in Fig. 23.

As shown in the figure, increasing the blast pressure can increase the extent of rock mass breakage around the blasthole, but is disabling to generate a continuous fracture plane. Furthermore, the restricted area in surrounding block of blasthole causes excessive failure of rock mass in the block and develops crushed zone and radial fractures to other directions than desired direction, which leads to damage to remained wall and instability of final face as well as remaining an irregular and rough surface. On the other hand, increasing the blasthole's diameter is another choice. In Fig. 24 rock breakage in a model with 0.1 m radius of blastholes is shown.

Increasing the radius to 10 cm increases the extent of failure, but still continuous fracture plane is not generated and the aim of pre-split blast is not achieved. Moreover, in this case damage to other directions is also excessive and remained wall is too fragmented which can affect stability of remained wall and may leads to instability of final wall. As a result of numerical modelling of pre-split blast in rock masses containing randomly polygonal joints, generation of a continuous controlled fracture plane is almost inaccessible and other controlling method should be applied at theses rock masses. In order to evaluate the effect of stresses distribution in surrounding blocks of a blasthole on rock breakage, 20 history points were place in 3 blocks around the blasthole. Fig. 25 illustrates variation of $S_{xx}$, $S_{yy}$ and $S_{xy}$ in the points. As shown in the figure, points located inside the block containing blasthole (marked with number 1) suffer intense stresses, while adjacent block (marked with 2 & 3) go under low values of stresses. The maximum magnitudes of $S_{xx}$, $S_{yy}$ and $S_{xy}$ for block 1 are 69.1, 47.14 and 19.787 in compression, respectively. While these values for block number 2 are 8.3, 6.1 and 2.568 and for block number 3 are 6.2, 5.03 and 2.117 all in compression, respectively. As a result, block 1 experienced very high compressive and failure is likely to occur, while the maximum stresses at block 2 and 3 is too low to be able to fragment the rock mass.

In the case of a rock mass with random jointing pattern (Figs. 14 and 15e) failure pattern and rock breakage is similar to randomly polygonal joints (Voronoi joints). In this case initiated fractures from blastholes are arrested by adjacent joints and frequent collision and reflection back toward individual blocks and leads to excessive breakage limited area between blastholes and adjacent joints. Joints act as a free face or a boundary between materials and cause energy wave reflection as well as attenuation. Fig. 26 shows a magnified view of rock breakage around blastholes. As shown in this figure, final face is rough and some areas (marked with brown arc) are likely to fall. The final face is at an acute angle and if the joint properties or filling material are of weak characteristics, then stability of remained wall will be a serious problem. Moreover, in rock masses with this kind of jointing pattern, if blast parameters such as holes diameter, explosive charge, burden and

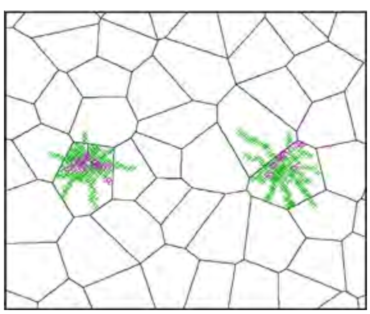

Fig. 22. Rock breakage pattern around blastholes in model with Voronoi joints.

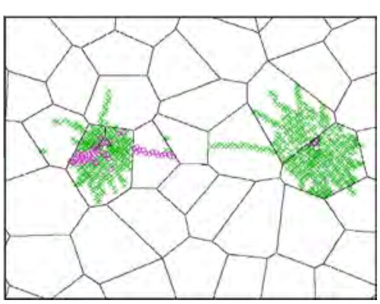

Fig. 23. Rock breakage with overloaded blastholes.

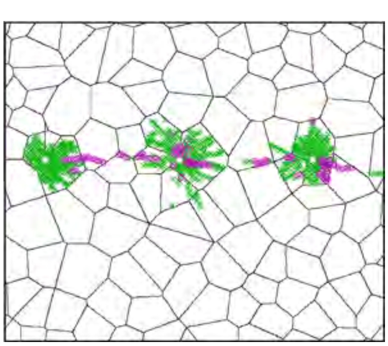

Fig. 24. Rock breakage in a model with 10 cm radius blastholes.

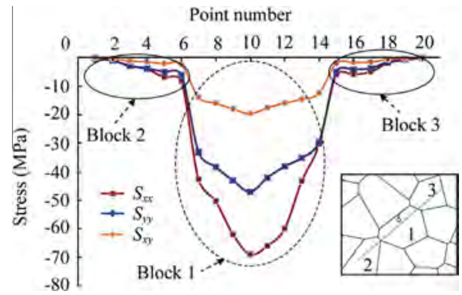


Fig. 25. Variation of $S_{xx}$, $S_{yy}$ and $S_{xy}$ in 20 points located at three surrounding block around a blasthole.

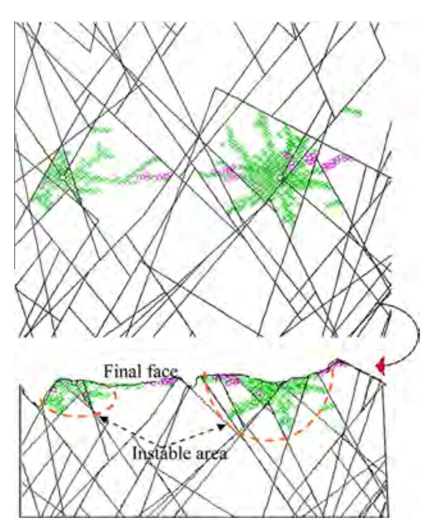


Fig. 26. Rock breakage around blastholes.

spacing between parameters are not selected properly, then pre-split blast may not be successful and final fracture plane will not generate.

## 8. Conclusions

The 2D dynamic commercial code was employed to study the presplitting blast method. The rock mass was considered to be a medium strength limestone typical of host rock in highway cuts in northern Iran. A Mohr-Coulomb material constitutive law was used to model the rock mass deformation and failure. Important stress components were measured at critical points (e.g., points between holes and along blasthole center line). The stress wave front and rock mass failure due to blast loading were shown. Two significant parameters, spacing and blast loading, were examined to better understanding of the presplitting mechanism. The numerical results show that spacing is the most significant governing parameters which control the final fracture plane's shape. Low spacing leads to generate a continuous and straight fracture which is desired scope. On the other hand, in low spacings, crushed zone is the dominate type of fracturing and areas between holes are crushed completely. When spacings are too far, a face that is generally rough in appearance will result and long fractures (e.g. incipiently fractures) are created in all directions which lead to damage to adjacent walls. In the other word, low spacing leads to increasing crushed zone around blastholes, but no cracks in y-axis and regular and flat boundary of remained wall. High spacing leads to low crushed zones, but longer fractures around blastholes, and irregular generated boundary and uneven remained wall. The second significant factor is blast loading. Conducted numerical study indicates that increasing in applied blast loading in too far spacings leads to generate a continuous fracture and low blast loads are not able to link fractures generated around blastholes. Moreover, high magnitudes of blast loading cause longer fractures around blastholes which lead to damage to adjacent walls. The distinct element simulations in jointed rock masses demonstrate great differences in fracture generation. On the other hand, different jointing patterns, as well, affect the breakage extent and damage to remained wall. At this study, five models with different jointing patterns were analyzed. The five models were jointing parallel to blastholes alignment axis, joints perpendicular to blastholes alignment axis, joints aligned at 45 degree orientated respect to blastholes alignment axis, rock masses with randomly polygonal joints (Voronoi joints) and random jointing. When joints are parallel to blastholes alignment axis, a continuous fracture plane is generated between blastholes easily, but wave reflection between two adjacent joints surrounding a blasthole leads to generate some radial fractures in opposite direction of main fracture plane and can lead to damage to remained wall. In the case of joints perpendicular to blastholes alignment axis, accurate spacing selection between blastholes is vital and generating fracture plane extremely depends on spacing. Because each joint acts as a barrier in front of wave propagation and does not allow energy wave to across the joint. When joints are aligned at 45 degree orientated respect to blastholes alignment axis, final face is generated in at acute angle and a rough remained wall will result. The reason is that wave reflection from orientated joint leads to generate acute fractures and linking between these fractures causes rough and irregular face. In the cases with randomly polygonal joints (Voronoi joints) and random jointing, the fragmentation process is almost similar. In both models, surrounding blocks of blastholes arrest fractures propagation to far distances and rock breakage is limited to close distances nearly to block diameter. On the other hand, frequent energy wave collision and reflection in an individual block containing blasthole leads to excessive failure of rock mass in the block and as a result, damage to remained block is severe. Furthermore, damage extension to remained face can lead to instability the remained wall which is undesirable in pre-split blast. Finally the study showed that more care should be done when pre-split blasting in jointed media. Accurate design of controlled pre-split blast depends on precise determination of controlled parameters such as borehole diameter, spacing between blastholes, explosive charge amount (blast load) as well as accurate measurement of joints physical and mechanical parameters such as spacing, dip and dip direction, spatial distribution and joint surface parameters.

364

## References


[1] Fourney WL, Holloway DC, Dally JW. Fracture initiation and propagation from a center of dilatation. Int J Fract 1975;11:1011–29.
[2] Fourney WL. Mechanisms of rock fragmentation in by blasting. In: Compressive rock engineering, principles, practice and projects. Oxford: Pergamon Press; 1993.
[3] Kaneko K, Matsunaga Y, Yamamoto M. Fracture mechanics analysis of fragmentation process in rock blasting. J Jpn Exp Soc 1995;58(3):91–9.
[4] Fourney WL, Dally JW, Holloway DC. Controlled blasting with ligamented charge holders. Int J Rock Mech Min Sci 1978;15:121–9.
[5] Nakagawa K, Sakamoto T, Yoshikai R. Model study of the guide hole effect on the smooth blasting. J Jpn Exp Soc 1982;43:75–82.
[6] Katsuyama K, Kiyokawa H, Sassa K. Control the growth of cracks from a borehole by a new method of smooth blasting. Min Safety 1983;29:16–23.
[7] Mohanty B. Explosive generated fractures in rock and rock like materials. Eng Fract Mech 1990;4:889–98.
[8] Mohanty B. Fracture-plane control blasts with satellite holes. In: Proceedings of the 3rd International Symposium on Rock Fragmentation by Blasting, Australia, 1990:407–12.
[9] Nakamura Y, Matsunaga H, Yamamoto M, Sumiyoshi K. Blasting methods for crack control by utilizing charge holders. J Jpn Exp Soc 1992;53:31–7.
[10] Ma GW, An XM. Numerical simulation of blasting-induced rock fractures. Int J Rock Mech Min Sci 2008;45:966–75.
[11] Nakamura Y. Model experiments on effectiveness of fracture plane control methods in blasting. Int J Blast Fragment 1999;3:59–78.
[12] Cho SH, Nakamur Y, Kaneko K. Dynamic fracture process of rock subjected to stress wave and gas pressurization. Int J Rock Mech Min Sci 2004;41:439.
[13] Nakamura Y, Cho SH, Yoneoka M, Yamamoto M, Kaneko K. Model experiments on crack propagation between two charge holes in blasting. Sci Technol Energ Mater 2004;65:34–9.
[14] Cho SH, Nakamura Y, Mohanty B, Yang HS, Kaneko K. Numerical study of fracture plane control in laboratory-scale blasting. Eng Fract Mech 2008;75:3966–84.
[15] Sharafisafa M, Mortazavi A. A numerical analysis of the presplitting controlled blasting method. In: Proceedings of the 45th US Rock Mechanics/Geomechanics Symposium, San Francisco, 2011.
[16] Sharafisafa M, Mortazavi A. Numerical analysis of the effect of a fault on blast-induced wave propagation. In: Proceedings of the 45th US Rock Mechanics/Geomechanics Symposium, San Francisco, 2011.
[17] Rathore SS, Bhandari S. Controlled fracture growth by blasting while protecting damages to remaining rock. Rock Mech Rock Eng 2007;40(3):317–26.
[18] Rossmanith HP, Uenishi K. The Cuña Problem-Reconsidered. In: Proceedings of the 12th International Conference of International Association for Computer Methods and Advances in Geomechanics, India, 2008.
[19] Lopez JC, Lopez JE. Drilling and blasting of rocks. Rotterdam: A. A. Balkema; 1995.
[20] Hemphill GB. Blasting operation. New York: Mc Graw Hill Inc; 1981.
[21] Atlas Powder Company. Explosives and Rock Blasting. Dallas: Atlas Powder Company, 1987.
[22] Khan GN. Discrete element modelling of rock failure dynamics. J Min Sci 2012;1(48):96–102.
[23] Aliabadian Z, Sharafisafa M, Mortazavi A. Investigation of the effect of in-situ stresses and loading rate on blasting induced fracture propagation. In: Proceedings of the 46th US Rock Mechanics/Geomechanics Symposium, Chicago, 2012.
[24] Paventi M, Mohanty B. Mapping of blast-induced fractures in rock. In: Proceedings of the 7th International Symposium on Rock Fragmentation by Blasting, Fragblast, Beijing, 2002:166–172.
[25] Bulson PS. Explosive loading of engineering. A history of research and a review of recent developments. London: E & FN Spon; 1997.
[26] Starfield AM, Pugliese JM. Compressional waves generated in rock by cylindrical explosive charges: a comparison between a computer model and field measurements. Int J Rock Mech Min Sci 1968;5:65–77.
[27] Duvall WI. Strain-wave shapes in rock near explosions. Geophysics 1968;18:310–23.
[28] Liu YQ, Li HB, Zhao J, Li RJ, Zhou QC. UDEC simulation for dynamic response of a rock slope subject to explosions. Int J Rock Mech Min Sci 2004;3(4):599–604.